

Solid state NMR investigation of photoresist molecular glasses including blend behavior with a photoacid generator†

David L. VanderHart,^a Vivek M. Prabhu,^{*a} Anuja De Silva,^b Nelson M. Felix^c and Christopher K. Ober^{*d}

Received 22nd September 2008, Accepted 28th January 2009

First published as an Advance Article on the web 5th March 2009

DOI: 10.1039/b816290e

We have examined four molecular glass (MG) materials that show promise as photoresists for extreme-ultraviolet (EUV) lithography. These glass-forming materials were investigated by proton and ¹³C solid state nuclear magnetic resonance (NMR) techniques in the *bulk* state as pure materials and as mixtures with (5 or 10) % by mass of the photoacid generator (PAG), triphenylsulfonium perfluorobutanesulfonate. The ¹³C techniques gave information about crystallinity, purity, and the qualitative existence of multiple phases. Proton studies focused on using spin diffusion to characterize the intimacy of mixing of the PAG and MG blends. The four MGs were largely aromatic materials containing several hydroxyl groups that were partially protected by *t*-butoxycarbonyl (*t*-BOC) groups. In two cases, this fraction was varied and the impact on mixing noted. Phase separation of the PAG into PAG-rich larger domains was never seen; the PAG was always finely distributed and the maximum size for any PAG clustering was estimated; however, in some cases, the average local concentration of PAG appeared to vary. Crystallinity was only seen associated with the underderivatized materials implying that the mixing of the PAG with any derivatized MG was not restricted by crystallization. It was also noted that some very strong hydrogen bonds exist in three of the four underderivatized materials and were eliminated or weakened upon partial derivatization with *t*-BOC.

Introduction

Photolithography remains the driving and enabling technology in the semiconductor industry to fabricate integrated circuits with ever decreasing feature sizes. Current fabrication facilities use chemically-amplified photoresists, *i.e.* complex and highly tuned formulations of a polymer film loaded with photoacid generators (PAGs) and other additives; the photoacid, activated by light exposure, catalyzes a deprotection reaction with the polymer that alters its solubility in a basic aqueous developer. Next-generation sources using extreme-ultraviolet (EUV) radiation with wavelength 13.5 nm are being developed to obtain improved resolution over deep-ultraviolet lithography at 193 nm. However, chemically amplified photoresist polymer materials may be reaching their fundamental limits as the feature dimensions approach the macromolecular size of the photoresist polymers. The goal of reducing line-edge roughness (LER), a metric for the ultimate resolution, to less than 5 nm is a challenge that must be resolved in order to extend high-volume production to features below 22 nm.

It was proposed that a small-molecule photoresist could be used instead of a polymer because it might form a surface with less roughness due to its smaller molecular size.^{1,2} In addition, such a discrete-sized material may eliminate issues specific to polymers such as polydispersity, chain entanglement and chain-end effects. This hypothesis has motivated the development of alternative material architectures such as small-molecule glasses, dendrimers, or single-component resists. Molecular-glass (MG) photoresists have shown promise, especially when incorporating design strategies which include efforts to increase the glass transition temperature (T_g) and suppress crystallinity. Crystallinity is undesirable because it would tend to lead to demixing.

The first reports of a chemically amplified molecular glass resist system were based on disk-like tri(hydroxyphenyl) molecules³ whose T_g s were relatively low, *i.e.* in the vicinity of 70 °C. The Ober group extended this work by designing a larger molecule with six phenolic groups, attached to the central benzene moiety, with hydroxyl substituents in alternating *meta* and *para* positions⁴ (PB-0 as shown in Fig. 1). This approach increased the T_g and simultaneously suppressed crystallization owing to the presence of two isomers. This model system, after being derivatized (protected) at the hydroxyl sites by acid-sensitive *t*-butoxycarbonyl (*t*-BOC) groups, was employed to achieve sub-50 nm resolution using electron beam lithography.⁵

Calix[4]resorcinarenes provide ring-like architectures and are synthesized via acid catalyzed reactions between resorcinols and acetaldehydes. By modifying the aldehyde or resorcinol starting materials, a variety of calix[4]resorcinarene derivatives can be prepared; often as a mixture of stereoisomers.^{6,7} The HR and tBR forms, shown in Fig. 1, were designed as both positive⁸ and negative tone photoresists.^{4,9} The HR-0 and tBR-0 systems were

^aPolymers Division, National Institute of Standards and Technology, Gaithersburg, MD, 20899-8541, USA. E-mail: vprabhu@nist.gov

^bDepartment of Chemistry and Chemical Biology, Cornell University, Ithaca, NY, 14850, USA

^cDepartment of Chemical and Biomolecular Engineering, Cornell University, Ithaca, NY, 14850, USA

^dDepartment of Materials Science and Engineering, Cornell University, Ithaca, NY, 14850, USA. E-mail: cober@ccmr.cornell.edu

† Electronic supplementary information (ESI) available: NMP affinity for underderivatized and derivatized HR, NMR evidence for crystallinity. See DOI: 10.1039/b816290e

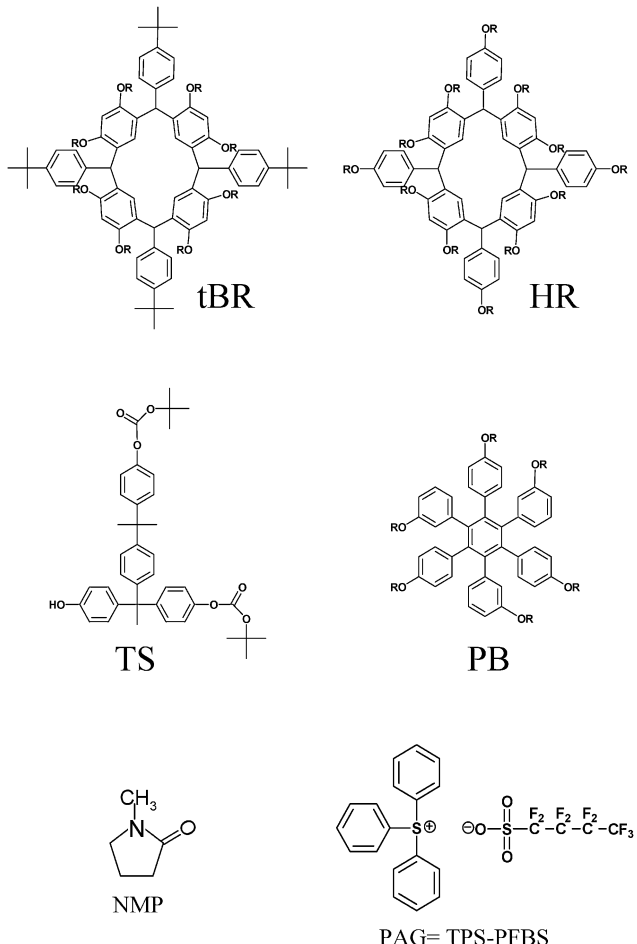


Fig. 1 Basic chemical structures, with acronyms, for the materials referred to in this paper (see also Table 1). Samples tBR-0, HR-0, TS-0 and PB-0 have R=H. Otherwise, the R groups are t-BOC groups, [*t*-butoxycarbonyl: *i.e.* $-\text{C}(=\text{O})\text{OC}(\text{CH}_3)_3$], substituting at levels listed in Table 1. t-BOC structures are illustrated on the TS structure at two of the three available hydroxyphenyl sites. In PB, the substituents around the central phenyl moiety alternate with *para* and *meta* hydroxyls. A second isomer is also present having one of the adjacent pairs in reverse order. These structural variations help to suppress crystallization of PB-0 and PB-100. The structure of the impurity, NMP, is also given.

converted into positive tone by protection of the hydroxyl groups with t-BOC. Two stereoisomers are reported for the HR-0 synthesis and one for the tBR synthesis.⁸ The HR and tBR^{10,11} systems show promise as next-generation materials as shown by sub 50 nm resolution by EUV lithography.^{12,13} Moreover, HR with 70% by mol t-BOC protection (HR-70) showed an improved LER of 4.6 nm (3σ) for 50 nm dense lines. These two structures have intrinsic differences in polarity since HR-70 has a polar hydroxyl functionality on each bridging phenyl ring, while tBR-70 has a non-polar *t*-butyl group. The optimal t-BOC protection between (60 and 70)% by mol was attributed to the balance of hydrophilic and hydrophobic content in the resist matrix that increased the T_g (>100 °C), improved substrate adhesion, and EUV exposure-dose sensitivity.

In addition to the resorcinarene systems, short-branched phenolic molecules based upon T-shaped (TS) molecules¹⁴ are

also promising materials based upon commercially available precursors. This MG photoresist showed sub-100 nm performance with both electron beam and EUV lithography. The main drawback was the low T_g (<70 °C) upon partial protection with t-BOC. However, this system served as a platform to design other high T_g materials based on its branched phenolic architecture.

These ring-like, disk-like, and short-branched architectures show promise as next-generation materials. A general problem when using these as photoresists, however, is to achieve an intimate dispersion of additives. Phase separation or component aggregation could reduce the ultimate resolution, especially if the characteristic cluster sizes are on the order of desired features. This paper probes the PAG and MG miscibility in the bulk state as a function of the three architectures and of t-BOC protection level. In a PAG and polymer blend system the entropy for mixing is reduced due to the presence of long chain molecules in the binary mixture. However, one expects an increase in the entropy of mixing between the MG and PAG molecule due to more comparable size.

Solid state proton nuclear magnetic resonance (NMR) spectroscopy has been shown^{15–19} to be a useful tool for probing the intimacy of mixing in blends of materials. The quantitative nature of proton signals and the high sensitivity of protons relative to other possible nuclei (*e.g.* ^{13}C) are important characteristics which direct us to techniques of proton observation. In particular the use of multiple pulse techniques, such as the MREV-8 sequence,^{20,21} provides a method of narrowing spectra greatly by eliminating dipolar interactions so that chemical shift effects dominate. The addition of magic angle spinning (MAS)^{22,23} narrows spectra further so that, using the combined technique,²⁴ CRAMPS (combined rotation and multiple pulse spectroscopy) spectra reflect the isotropic values of the chemical shift, just as is the case in liquid state NMR. Achievable resolution of about 1 ppm to 2 ppm, however, is only modest, compared to liquid state resolution, for most amorphous solids. Nevertheless, that resolution level is often sufficient for differentiating signals from chemically distinct components. We make use of the foregoing techniques in a multi-period pulse sequence^{15,16} in which the first fixed period is devoted to establishing a proton-polarization gradient between components and the ensuing variable “spin-diffusion” period is a time of full dipolar couplings where polarization is free to diffuse, approaching, in the case of good mixing, sample-wide spin equilibrium. In the final period, CRAMPS spectra are collected, each of which indicates the progress of spin diffusion during the variable t_{sd} period. An extended network of homonuclear dipolar couplings facilitates spin diffusion²⁵ which really is the diffusion of polarization and not of the spins themselves. Such spin diffusion is a constant process; however, it is only detected in the presence of a polarization gradient. In the spin diffusion experiment, information about the intimacy of mixing of the components is extracted²⁶ from the behavior of the polarization as a function of this latter spin diffusion time, t_{sd} .

In this work, we focus on mixing of the PAG in the MGs in bulk samples. Given that use of photoresists in manufacturing is exclusively a thin film application, we offer a few perspectives for applying our bulk results to thin films. Owing principally to our limited resolution, our bulk-state test is sensitive to the presence of impurities; hence, we really cannot tolerate significant residues

of solvent or other minor impurities. In turn, this means that the solvents we use to prepare bulk solvent-free samples typically have a relatively high volatility, whereas one tends to use solvents with somewhat lower volatility for spin coating of thin films. *The unambiguous correspondence of the NMR results to thin film preparations is only in the specific outcome that the NMR results show intimate mixing.* If that is the case, then we argue that the PAG and MG are thermodynamically compatible. We recognize that since the solvent in the preparation of the bulk solid is withdrawn slowly, any thermodynamic incompatibility would result in detectable phase separation. In contrast, if separate

phases are found, with one rich in PAG, it is possible that thermodynamic incompatibility is just one of the possibilities, the other likely choice being differential solubility of PAG and MG in the solvent. If the latter is true, then thermodynamic compatibility of PAG and MG remains a possibility, even though each particle of the bulk solid would consist of a continuously changing composition as one moves from the inside to the outside. Finally, it is also clear that the bulk state does not permit any significant expression of surface-affinity effects which can occur in thin films and result in concentration gradients near the surface, even in the presence of bulk-state thermodynamic compatibility.^{27–30}

Table 1 Composition and abbreviations for each sample; see Fig. 1 for chemical structures

Sample acronym	Main component ^a	t-BOC protection level of OH (% by mol of original OH sites)	% By mass ^b	% By mass ^b of TPS-PFBS
tBR-0	4tBPCR-0	0	100	
tBR-70	4tBPCR-70	70	100	
tBR-25	4tBPCR-25	25	100	
5tBR-70	4tBPCR-70	70	95	5
10tBR-70	4tBPCR-70	70	90	10
5tBR-25	4tBPCR-25	25	95	5
HR-0	4HPCR-0	0	100	
HR-70	4HPCR-70	70	100	
HR-25	4HPCR-25	25	100	
5HR-70	4HPCR-70	70	95	5
10HR-70	4HPCR-70	70	90	10
5HR-25	4HPCR-25	25	95	5
PB-0	HHPB-0	0	100	
PB-100	HHPB-100	100	100	
5PB-100	HHPB-100	100	95	5
10PB-100	HHPB-100	100	90	10
TS-0	BHEDBP -0	0	100	
TS-75	BHEDBP -75	75	100	
5TS-75	BHEDBP -75	75	95	5
10TS-75	BHEDBP -75	75	90	10

^a Abbreviations and chemical correspondences: **TPS-PFBS** = triphenylsulfonium perfluorobutanesulfonate, **t-BOC** = *t*-butoxycarbonyl (t-BOC) [$\text{C}(=\text{O})-\text{O}-\text{C}(\text{CH}_3)_3$] (replaces the hydroxyl hydrogen in protected molecules), **4tBPCR-n** = 4-tertiary-butylphenyl calix[4]resorcinarene, **4HPCR-n** = 4-hydroxy-phenyl calix[4]resorcinarene, **HHPB-n** = hexa[(*m*- and *p*-hydroxyphenyl]benzene, **BHEDBP-n** = a “T”-shaped molecule: 4-[4-[1,1-Bis(4-hydroxyphenyl)ethyl]]-R,R-dimethylbenzylphenol, *n* = % t-BOC protection. ^b These % by mass values ignore impurity levels.

Results and discussions

Determination of average protection levels

The average derivatization (protection) levels were determined by thermogravimetric analysis (TGA) as shown in Table 2. Also shown in Table 2 are the protection levels deduced from solid-state proton nuclear magnetic resonance lineshapes. We will compare both assays in our discussion of the NMR spectra. The distribution in number of t-BOC groups per molecule is not available from the foregoing measurements. Matrix-assisted laser desorption ionization mass spectrometry measurements at the National Institute of Standards and Technology (NIST), reported separately, generally indicate broad distributions for these resorcinarenes.³¹

Spin diffusion spectra of mixtures

Fig. 2 is an example of a set of CRAMPS spin diffusion spectra obtained from the 10tBR-70 sample containing 10% by mass of the PAG triphenylsulfonium perfluorobutanesulfonate (TPS-PFBS), where the CSBSD (chemical shift based spin diffusion¹⁵) has been employed. When referring to the PAG concentration it will be implied as % by mass from this point forward, unless otherwise noted. The initial polarization gradient formed in this experiment is a sinusoidally varying function across the proton CRAMPS spectrum. The first thing evident in comparing the equilibrium spectra, 2A and 2B, is that the expected signal strength of the PAG protons is exceedingly weak, relative to the tBR-70 protons. In fact, 2B is amplified vertically $\times 4$. Based on composition, the expected fractional intensity of the PAG

Table 2 Percentage of original hydroxyl sites occupied by t-BOC in the protected MGs: thermogravimetric analysis^a (TGA) and CRAMPS-NMR lineshapes

Sample	Target percentage (%)	Theoretical mass loss (%) ^b	Experimental TGA mass loss (%)	TGA estimate (%) ^c	NMR estimate (%) ^d	T _g (°C)
tBR-25	25	16	21	33 (2)	36 (4)	
tBR-70	70	36	37	72 (2)	61 (4)	
HR-25	25	26	31	30 (2)	22 (6)	
HR-70	70	50	50	70 (2)	66 (5)	
TS-75	75	35	34	73(2)	92 (4)	60
PB-100	100	49	49	100 (2)	100 (3)	105

^a TA Instruments Q500 using a heating rate of 10 °C/min under N₂. ^b Based on the thermal loss of the t-BOC group assuming the target percentages.

^c Standard uncertainties are shown in parentheses; they are based on a TGA measurement uncertainty that is 1% of original mass. ^d Based on integration of the “aromatic” region (aromatic plus hydroxyl protons) of CRAMPS spectra. Standard uncertainties are given in parentheses. The HR sample has higher uncertainty owing to the presence of the impurity, NMP, whose concentration was deduced from ¹³C spectra.

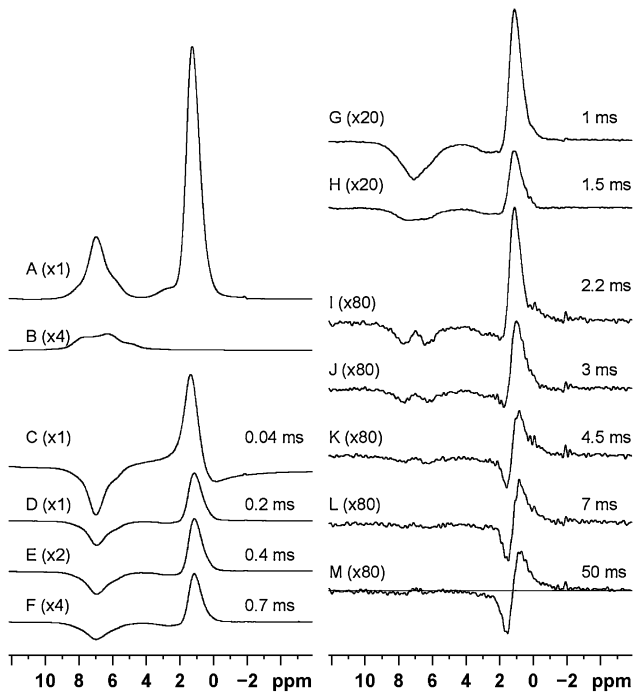


Fig. 2 300 MHz proton CRAMPS (combined rotation and multiple pulse spectroscopy) spectra related to spin diffusion of 10tBR-70. A: equilibrium lineshape; B: crystalline TPS-PFBS at a level 4 times that expected in 10tBR-70; C to M: “zero-integral” spin diffusion spectra at indicated spin diffusion times. Each latter spectrum is modified slightly by adding a scaled amount of lineshape A, such that total integrals are zero (such spectral addition preserves gradients). Spectral multiplication factors are also shown every time the latter factor changes. The aliphatic region is from about (0 to 5) ppm; the aromatic region is from about (6 to 9) ppm. The initial state features a negative aromatic polarization (arising from the MG plus the PAG) of much larger magnitude than the corresponding positive aliphatic polarization (MG only). Most of the initial intensity change over the first 3 ms is due to equilibration of aromatic and aliphatic protons in the 10tBR-70 component. Disappearance of intensity in these spectra means that sample-wide spin equilibration has been reached within the signal-to-noise for the PAG protons after about 4.5 to 7 ms, thereby signaling intimate mixing. Apparent dispersive character of aliphatic line is an artifact of the method given the relatively narrow aliphatic proton line associated with *t*-butyl protons; the important issue is the simultaneous zero total integrals of both aromatic and aliphatic regions. Note the good sensitivity in that proton spectra still have a small noise level after an 80 fold vertical amplification.

protons, relative to all protons, is 3.85%. Spectrum 2B is also distorted in the sense that the only spectrum of the pure PAG which we can get is that of the crystalline state; whereas, if the PAG is dispersed, we expect a smoother, less defined resonance profile, even though the spectral position should be similar to that of the crystalline state. In Fig. 2, spectra C through L represent modified, “zero-integral” spin diffusion spectra at the indicated spin diffusion times (t_{sd}) with the indicated vertical amplification factors. The figure caption gives more details about the how the “zero-integral” spectra are generated. Basically, the modification preserves all polarization gradients associated with the unmodified spin diffusion spectra while offering the simplifying visual criterion that, *when sample-wide spin equilibrium is finally achieved, signals from each type of proton should ideally*

vanish. i.e., have an integral of zero. In Fig. 2, note the good signal-to-noise ratio, even for an amplification of $\times 80$.

Before offering the qualitative interpretation of Fig. 2, we list the following definitions and rules: (a) for a set of spins, *polarization* relates to the average projection, *per spin*, along the applied magnetic field; its corresponding *magnetization* is proportional to the product of polarization and the number of such spins, (b) spin diffusion, in the absence of longitudinal relaxation, preserves total magnetization, and (c) spin equilibrium among all protons is defined as a state where all proton polarizations are equal for each distinguishable set of protons. Thus, spectra 2C through 2M illustrate the following: (1) the initial condition produced by the gradient preparation features a negative aromatic (≈ 5 ppm to 9 ppm) and a comparable positive aliphatic (≈ 0 ppm to 5 ppm) *magnetization*; however, since the aromatic signal in 2A is much weaker than the aliphatic signal, the corresponding aromatic *polarization* in 2C is much more strongly negative than the aliphatic polarization is positive. (2) Most of the increase in aromatic intensity and the corresponding decrease in aliphatic intensity is associated with spin equilibration between the aromatic and aliphatic protons within the tBR-70 component. Owing to known physical proximity, one expects nearly complete spin equilibration between all protons associated with that component over a t_{sd} of 2 ms to 3 ms and we will presently discuss that process in Fig. 3. (3) As an indication of the quality of mixing of PAG and tBR-70, one looks for the PAG signal to fade away over t_{sd} values longer than 3 ms. In Fig. 2L, at $t_{sd} = 7$ ms, that aromatic signal is already fading into the noise, a condition that holds true for all longer times as well.

In Fig. 3 the results of the control experiment on tBR-70 are shown. The idea of this experiment is to generate a polarization gradient between aliphatic and aromatic protons of the pure MG and then measure how long it takes for those protons to reach a common polarization level (spin equilibration). This measurement gives a value of t_{sd} beyond which it is safe to assume that remaining polarization gradients in the MG/PAG sample can be interpreted as gradients between average PAG and average MG polarizations. Lineshapes similar to those of Fig. 2 are seen with all expected changes relating to the equilibration of the aromatic and aliphatic polarizations. Lineshape changes are still happening between 2 ms and 3 ms as can be seen most easily in the aromatic region; however, changes are insignificant beyond 3 ms. Thus, for interpreting the data of Fig. 2, we must wait until 3 ms before the aromatic lineshape will allow a relatively clean determination of the PAG contribution.

One feature of Fig. 3 is that the criterion that the intensity vanishes when spin equilibrium returns is not seen since both aromatic and aliphatic intensities remain, albeit both aromatic and aliphatic lines appear to be dominantly dispersive rather than absorptive, *i.e.*, they each have near-zero-integrals and that is the main thing which indicates spin equilibration. The dispersive character is present because the static field, \mathbf{B}_0 , and the rf field, \mathbf{B}_1 , each have modest gradients associated with them, such that the initial, imposed polarization gradient changes slightly across the sample. Because of this, even though MG and PAG protons may come to full equilibrium locally, a gradient of polarization, *the same for all PAG and MG resonances*, persists. This persistent gradient does not disappear *via* spin diffusion on the experimental timescale owing to the large, sample-wide

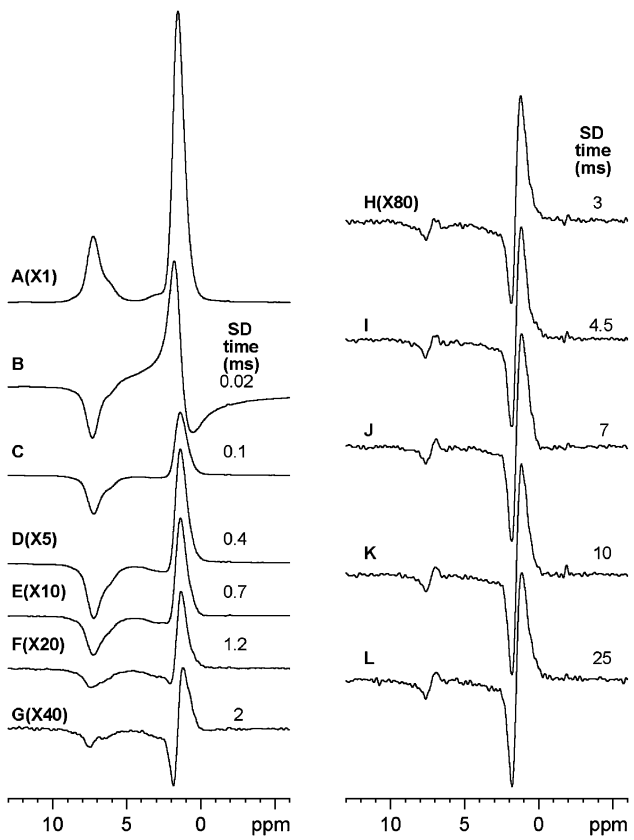


Fig. 3 Spin diffusion CRAMPS spectra of tBR-70 having to do with the time required to achieve internal spin equilibrium between aliphatic and aromatic protons within the tBR-70 itself. A: equilibrium spectrum; B to L: zero-integral spin diffusion spectra with vertical amplification factors. Lineshapes quit evolving at about 3 ms. Weak dispersive character of the lineshapes at longer times is an artifact of the method, and is similar to that seen in Fig. 2. The zero-integral nature of both resonances indicates that while aromatic/aliphatic polarizations have equilibrated locally, small variations in the equilibrated mean polarization exist over much larger distances (>100 nm) than can be accessed by spin diffusion.

distances over which the gradient is defined. Thus, this persistent gradient is a nuisance even though it is small, *i.e.*, positive and negative aliphatic amplitudes in 3L are less than 0.5% of the peak amplitude in 3A. However, since we always use a fixed phase correction for each spectrum, the criterion for the return to spin equilibrium of all constituents locally remains that the total integrals of each component go to zero. For example, one can see that in 3G this criterion is not met, while in 3H it is very close to being met. One other thing about the persistent gradient is that the narrower the intrinsic linewidth, the more intense, relative to the Boltzmann-equilibrium amplitude, will be these ‘dispersive’ amplitudes. Hence, since the aromatic line is intrinsically wider than the aliphatic line in Fig. 3A, it follows that in spectra 3H to 3L, peak-to-peak amplitude ratios of the dispersive aromatic and aliphatic lines are smaller than the corresponding peak amplitude ratio in 3A.

Based on the foregoing interpretation, the tBR-70/PAG spin equilibration in Fig. 2 takes place in a time (7 ms) very comparable to that of internal tBR-70 spin equilibration (3 ms) and this fact qualitatively implies intimate mixing. What remains to be

done is to put this result on a more quantitative footing, particularly in view of the fact that the PAG signal is inherently weak and we must consider the threshold of detection of the PAG signal and how that introduces uncertainty into the analysis.

Proof that the PAG exists in the mixed samples

The analysis and interpretation of the spin diffusion data for the mixtures depends on the presence of the PAG at a concentration approximately that anticipated from the stoichiometries of the mixed precursor solutions. Experimentally the samples were made and collected in such a way that there should be negligible loss of sample; however, there is, in principle, a small chance that if extensive phase separation of the PAG occurs and if there are corresponding PAG-rich solid particles with grain size sufficiently different from the MG-particle grain size then the overall sampling for NMR analysis could depart somewhat from average sample stoichiometry. Our methods for verifying stoichiometries for each mixed sample relied on comparisons of spectra of each mixture with spectra of the corresponding pure MG. For most samples, where impurities were not an issue, this could be done quantitatively using proton CRAMPS spectra where an increase in the aromatic intensity for the mixture, relative to the MG, could be monitored. When impurities were present, less quantitative ^{13}C spectra were compared and an increase in the protonated-aromatic ^{13}C intensity was monitored. Proton and ^{13}C results, respectively, verified expected compositions within error limits of 20% and 30%. This was taken by us to be adequate proof that there were no important issues regarding sampling and phase separation. The results to be discussed verify the lack of such troublesome phase separation. A final comment about compositional assumptions is that the spin diffusion analysis we use is robust in tolerating compositional deviations; yielding a multiplicative correction factor (proportional to the ratio of assumed to actual PAG concentration) for each spin diffusion datum.

A few perspectives on the interpretation of spin diffusion data

We mentioned that intermolecular spin diffusion between MG and PAG in Fig. 2 is qualitatively indicative of intimate mixing because it takes place on a timescale just a few times that of the time it takes for the *intramolecular* equilibration process between aromatic and aliphatic protons within the MG itself. There is one important difference between the processes of intramolecular and intermolecular spin equilibration in these cases, *i.e.* for the MGs, the fraction of aromatic protons is at least 20% while for the PAG, the fraction of PAG aromatic protons in the mixture is most often much smaller and in the 2% to 4% range (see Table 3). An easy way to think about the significance of this difference is to think about the spin diffusion experiment, in the absence of relaxation to the lattice, as an adiabatic experiment where the total magnetization is preserved. Then, the final average polarization, P_f , is simply the total magnetization divided by the total number of spins. This is expressed in eqn (1):

$$P_f = (M_\alpha + M_\beta)/(N_\alpha + N_\beta) = (P_{i\alpha}N_\alpha + P_{i\beta}N_\beta)/(N_\alpha + N_\beta) \quad (1)$$

Table 3 Spin diffusion results for all mixtures of PAG and molecular glasses along with the theoretical fraction of PAG protons for each mixture based on the given stoichiometries

Sample	Theor. ^a fraction of PAG protons	$\Delta M_s(t_{sd})^b$					Remarks (abbreviations: Ar/Al : aromatic/aliphatic; Eq. : equilibration; SD : spin diffusion; inhomo : inhomogeneous; dist : distribution; imp : impurity)
		$t_{sd} = 3$ ms	4.5 ms	7 ms	10 ms	25 ms	
tBR-70							Ar/Al spin Eq. in 3 ms
5tBR-70	0.0186	.08	.06	.055	.044	.033	Inhomo dist of PAG/MG exists, but not thermodynamic, based on well behaved 10tBR-70; no NMP imp.
10tBR-70	0.0385	.053	.026	.014	.012	<.010	Intimate mixing
tBR-25							Ar/Al spin Eq. in 4 ms
5tBR-25	0.0190	.070	.020	<.010	<.010	<.010	Intimate mixing
HR-70							Ar/Al spin Eq. in 4 ms
5HR-70	0.0217	.064	.028	.018	.012	.008	Intimate mixing. NMP present at a level ≈ 2 NMP molecules per 3 molecules of MG; NMP intimately distributed; also weak implied support for good mixing of the two types of derivatized isomers.
10HR-70	0.0448	.062	.035	.023	.014	.008	
HR-25							NMP has $(15 \pm 3)\%$ of total ^{13}C intensity; Ar/Al spin Eq. not quite fully reached; SD lineshape stabilizes at 7ms.
5HR-25	0.0247	.150	.102	.053	.039	.030	NMP has $(12 \pm 3)\%$ of total ^{13}C intensity; Ar/Al spin Eq. not quite fully reached; three possible reasons for non-Eq.: a) inhomo dist of PAG/MG; b) inhomo dist of NMP, and c) some segregation in MG based on extent of derivatization. a) is considered least likely since HR-25 behaves similarly.
PB-100							Ar/Al spin Eq. in 4 ms
5PB-100	0.0217	.070	.053	.047	.042	.033	Negligible imp's; inhomo dist of PAG/MG; equal behavior of both samples points to differential solubility, rather than thermodynamic incompatibility.
10PB-100	0.0447	.066	.052	.045	.042	.035	
TS-75							Ar/Al spin Eq. in 3 ms
5TS-75	0.0194	.075	.032	.024	.010	.01	Intimate mixing for both samples
10TS-75	0.0402	—	.026	—	.012	—	

^a Based on given stoichiometries in Table 1 and no impurities. ^b $\Delta M(t_{sd})$ is the scaled deviation of aromatic PAG polarization from sample-wide spin equilibrium (see text). Its maximum range is from an initial value of 1.0 to 0.0, provided spin equilibrium is achieved.

where the M 's are magnetizations, the P_i 's are initial polarizations, the N 's are the numbers of spins and α and β refer to each of the two components. Eqn (2) also incorporates the conservation of magnetization, namely, that

$$\Delta M_\alpha = -\Delta M_\beta \text{ or } \Delta P_\alpha N_\alpha = -\Delta P_\beta N_\beta \quad (2)$$

where the “ ΔM ” and “ ΔP ” quantities are differences between initial and final (or intermediate) magnetizations and polarizations, respectively. For the MG/PAG mixtures, where the PAG protons represent, at most, 5% of the total number of protons, eqn (2) indicates that almost all of the polarization change is associated with the PAG protons. In addition, as the number of PAG molecules diminishes, the probability that a PAG molecule, in a well dispersed system, is completely surrounded by MG molecules becomes higher. Thus, this change in nearest neighbor statistics tends to speed up the polarization change associated with the PAG protons in a dilute environment. Without going into a lot of detail, an important perspective on the data is that when the dilute PAG is dispersed on a molecular basis, one will see a rapid and large initial change in its polarization.

About spin diffusion plots

Quantitative analysis for spin diffusion spectra like that of Fig. 2 has been discussed previously^{19,26} and we will only mention a couple of key aspects. First, based on having done similar experiments on the pure components, *i.e.* each MG and the pure PAG, we have a good idea about the initial, average proton

polarization levels for the aliphatic and aromatic protons in the experiment on the mixture. We use these levels as input, along with the data, in order to deduce the quantity, $\Delta M_s(t_{sd})$ as a function of the spin diffusion time. Basically, $\Delta M_s(t_{sd})$ is a scaled quantity, proportional to the difference between the actual *average* PAG polarization and that final *average* PAG polarization characterizing the ideal state of full *spin equilibration of MG and PAG*. The scaling is such that if no spin diffusion between MG and PAG protons occurs (*e.g.* for complete phase separation into large domains) then $\Delta M_s(t_{sd}) = 1.0$. On the other hand, when complete spin equilibration between PAG and MG protons occurs, then $\Delta M_s(t_{sd}) = 0$. In a mixed system where spin diffusion is effective and the process of spin equilibration goes to completion, $\Delta M_s(t_{sd})$ will change from 1.0 to 0.

Normally, in a two phase system, one gets some idea of the domain sizes from the initial slope of a $\Delta M_s(t_{sd})$ vs. $(t_{sd})^{1/2}$ plot.^{26,32} In our case, we cannot capture this initial slope owing to two issues, namely, (a) the spectral overlap of MG and PAG resonances and (b) the fact that the initial polarization gradients, based on chemical shifts, produce gradients both within and between protons of the PAG and MG (this is particularly true for the latter which includes both aromatic and aliphatic protons). The existence of polarization gradients within a component's protons means that the equilibrium lineshape for that component will not apply; hence, lineshape deconvolutions are not justified until such intra-component equilibrium is achieved. Thus, information about the initial slope is lost while waiting, mainly for the aromatic and aliphatic polarizations from the MG, to come to equilibrium (≈ 3 ms for these MGs as determined by experiments

like that shown in Fig. 3). Hence, only the tail of the equilibration curve ($t_{\text{sd}} \geq 3$ ms) can be determined after one makes the following assumptions: (a) there is full spin equilibration of all the MG aromatic and aliphatic protons for $t_{\text{sd}} \geq 3$ ms (as will be shown, this is true for most MGs); (b) the PAG is present at the overall concentration determined from the mixing stoichiometry and (c) the initial average proton polarization levels of the MG and the PAG are known (they are measured on the pure materials). Thus, rather than plot only the longer-time tails of the data, we collect in Table 3 the values of $\Delta M_s(t_{\text{sd}})$ for 5 values of $t_{\text{sd}} \geq 3$ ms for the various mixtures of PAG and MGs. The existence of impurities, as is true of some of our samples, represents yet another complication, especially if the impurity protons outnumber those of the PAG, since incomplete equilibration can also arise from the inhomogeneous distribution of the impurity.

The main conclusion to be drawn from Table 3 is that spin diffusion, at $t_{\text{sd}} = 3$ ms (where further *internal* spin equilibration within the MG should be small or negligible), has taken the PAG polarization through at least 85%, and, most of the time, at least 92% of the change required to reach sample-wide spin equilibrium. In other words, most of the major changes in PAG polarization occur over a time very similar to that required for intramolecular spin equilibration on the MG molecules. Furthermore, for those samples labeled in Table 3 as intimately mixed, $\Delta M(t_{\text{sd}})$ is generally near 0.01 at $t_{\text{sd}} = 7$ ms. At least qualitatively, a difference of a factor of 2 or 3 in the time required for achieving intramolecular MG equilibrium *versus* intermolecular PAG/MG equilibration is suggestive of intimate mixing between PAG and MG. However, we must make the argument more quantitative.

Maximum PAG domain size: intimately mixed samples

In order to quantify the real meaning of “intimate mixing,” one would like to measure the entire spin diffusion curve, especially the initial slope, and perform some calculations based on some assumed diffusion constants and PAG dispersions. However, since we do not have the complete curves in this case, we shall choose a semiquantitative approach. By analogy to other, more detailed data, we estimate the initial slope and calculate the diameter, d_{PAG} , of a PAG spherical domain, assuming, as a worst case, that the PAG wants to phase separate. By this exercise we generate, for those samples showing intimate mixing, a *conservative* upper limit to the size of PAG aggregation, consistent with what we observe (Table 3) in the tail of the more well behaved spin diffusion plots.

Our approach is to refer to a previous unpublished and more detailed spin diffusion measurement that we made while investigating mixing of the present PAG with polymeric matrices related to 193 nm photoresists. Fig. 4 shows the spin diffusion plot for a 95/5 blend of PHAdMA/TPS-PFBS (PHAdMA = poly(2-hydroxyadamantyl methacrylate). The big advantage of this system is that the only aromatic protons in this sample are the PAG protons; hence, the PAG polarization can be monitored at all spin diffusion times. When we compare the tail of this curve with those of the samples we have labeled intimately mixed in Table 3, we find that comparable $\Delta M(t_{\text{sd}})$ values for our samples occur at t_{sd} values about 3 times longer than for the PHAdMA/TPS-PFBS. The suggestion is therefore strong that the intercept

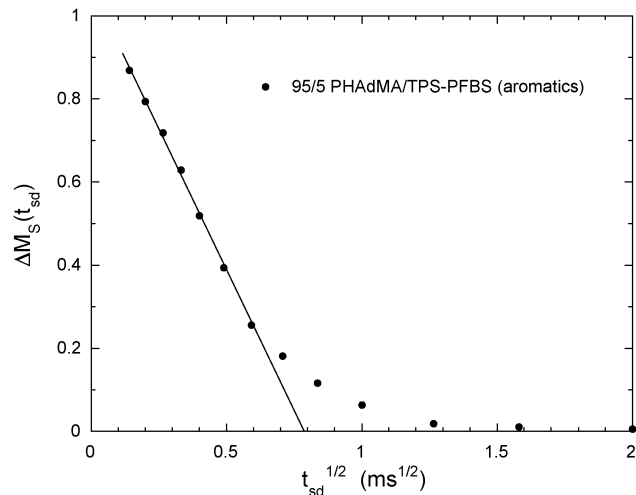


Fig. 4 Spin diffusion plot for the 95/5 PHAdMA/TPS-PFBS system. The decay from 1 ms on to longer times mimics the average decay seen for the “intimately mixed” samples in Table 3, provided that the times indicated here are multiplied by a factor of 3. Uncertainties are given by the symbol size. The initial slope is the solid line and its intercept with the abscissa gives $(t_{\text{sd}}^*)^{0.5}$.

of the initial slope with the abscissa, $(t_{\text{sd}}^*)^{0.5}$, which is $(0.79 \pm 0.03) \text{ ms}^{0.5}$ in Fig. 4, should be multiplied by $3^{0.5}$ to obtain $(t_{\text{sd}}^*)^{0.5}$ for our samples, *i.e.* $(t_{\text{sd}}^* = 1.88 \pm 0.15) \text{ ms}$. We can use this value to estimate the diameter, d_{PAG} , of a spherical domain of a very minor phase using the approximation²⁶

$$d_{\text{PAG}} \approx 6(Dt_{\text{sd}}^*/\pi)^{0.5} \quad (3)$$

where D is an effective diffusion constant for the system. The diffusion constant we ascribe¹⁸ to the proton-rich, glassy PHAdMA, whose measured Bloch-decay proton linewidth is $(48 \pm 2) \text{ kHz}$, is $0.8 \text{ nm}^2/\text{ms}$. In contrast the corresponding linewidths of the blends under current investigation are all $(14 \pm 1) \text{ kHz}$, except for the low t-BOC derivatized HR-25 and tBR-25 samples whose linewidths are $(18 \pm 1) \text{ kHz}$. The difference in linewidths between PHAdMA and these MGs is mainly a result of the motional averaging of the preponderant *t*-butyl groups in our MGs. Exactly, the dependence of D on the matrix linewidth is debatable and depends on the detailed distribution of the protons; however, a reduction from that of PHAdMA by a factor of 2 is a conservative estimate, in our opinion. Moreover, such a reduction is consistent with the length of time, 3 ms or 4 ms in our samples, for the intramolecular spin equilibration within the matrix molecules. This is at least a factor of 2 longer than in other glassy materials, *e.g.*, poly(styrene),³³ whose linewidth is $(35 \pm 2) \text{ kHz}$ and whose comparable intramolecular equilibration time is $(1.4 \pm 0.2) \text{ ms}$. By substituting $D = 0.4 \text{ nm}^2/\text{ms}$ into eqn (3) gives $d_{\text{PAG}} = 2.9 \text{ nm}$. Even if this estimate of the spherical diameter of any separated PAG phase were off by 30%, the maximum spherical diameter of any phase separated region would be 3.8 nm, *i.e.*, still relatively small. Such a volume would contain about (40 to 45) PAG molecules. In order to get a crude idea of the mean separation between such domains, suppose the volume fraction of PAG was 0.04, the spherical diameter of the PAG domain was 3.8 nm, and the PAG was arranged on a regular

body-centered cubic lattice, then the expected separation between the centers of the spheres would be about 10 nm. In that case, the uniformity of reaction of the PAG with the host matrix would appear to depend on there being a radius, much larger than 5 nm, associated with the diffusion distance for a PAG molecule during the critical post exposure baking cycle. In practice, estimates of the distance traveled by the photoacid depend strongly on photoresist and post exposure baking conditions. In model poly(hydroxystyrene-co-tertbutylacrylate) photoacid diffusion lengths between 1 nm and 10 nm were observed³⁴ with TPS-PFBS and an 11 nm radius of gyration of the deprotection volume was observed³⁵ in poly(*t*-butoxy carbonyloxystyrene) with the PAG, di-*t*-butylphenyl iodonium perfluoroctanesulfonate. For PAG diffusion distances like that, a 10 nm separation between PAG domains seems coarse and could have an impact on the local uniformity of reaction. Note, however, that the 3.8 nm PAG diameter is a worst case scenario for phase separation and we cannot dismiss the other possibility that the PAG is dispersed on a molecular basis.

Given that these samples were formed by a modestly slow evaporation of the solvent, the idea that domains, rich in PAG and as small as 3.8 nm in diameter, would form based on some thermodynamic incompatibility, is implausible to us. Such small domains would have too much surface area and would be too costly, energetically. Thermodynamic incompatibility should, in our opinion, lead to the establishment of much larger domains. Hence, *these experiments prove the thermodynamic compatibility of TPS-PFBS with those MGs in Table 3 which are labeled as having intimate mixing.*

The compatibility of this PAG with these and other systems we have studied, including non-aromatic systems such as PHAdMA, is an intriguing subject in itself since the PAG is a salt and includes perfluorinated moieties as well as very polar moieties while the MG's lack fluorination but do possess some polarity associated with the *t*-BOC carbonyls and the residual hydroxyls. The interfacial energies would probably depend on the direction of approach of a matrix molecule to the PAG molecule. In this spirit, we emphasize that included in our concept of thermodynamic compatibility is the *possibility* that thermodynamic compatibility with these MGs may not necessarily imply the dispersion of *individual* PAG molecules into a solid solution with the MGs. Rather, for the purpose of lowering interfacial energies, it is conceivable that a few, maybe 3 to 6, PAG molecules might cluster together, largely sequestering those portions of the PAG molecule with least favorable interactions while optimizing the availability of those groups that interact most favorably with the MG's. The existence of such a modified dispersion of PAG would depend on the energetics of small-cluster formation more than offsetting the corresponding entropy decrease. Certainly, the experiments reported herein are not capable of proving or rejecting this possibility within the concept of thermodynamic compatibility.

Samples with slower approaches to spin equilibrium

The samples exhibiting a slower approach to equilibrium than would be expected for intimate mixing are 5HR-25 and, to lesser but similar extents, 5tBR-70, 5PB-100 and 10PB-100.

The slowest rate of approach to spin equilibrium for the 5HR-25 sample is accompanied by a substantial decrease in $\Delta M(t_{sd})$ in

the interval from $t_{sd} = 3$ ms to 7 ms. The pertinent question is whether this signals a clustering of the PAG into larger and inhomogeneously distributed domains or whether there is some other, more plausible explanation. In this case, there are two other reasonable possibilities. First, this sample contains residual 1-methyl-2-pyrrolidinone (NMP), as reflected in the ^{13}C spectra, where $(12 \pm 3)\%$ of the ^{13}C intensity arises from the NMP carbons. Since the NMP has only aliphatic carbons, an inhomogeneous distribution of NMP could easily be responsible for preventing sample-wide spin equilibration. Secondly, given that the derivatization of this sample is low, it is possible, in principle, that there is some phase segregation based on the degree of substitution on each molecule; such segregation would affect the aromatic/aliphatic ratio locally. In choosing a plausible explanation for the 5HR-25 data in Table 3, we appeal to the results of our baseline spin diffusion measurement on the HR-25 sample where we checked on the time dependence of spin diffusion between aliphatic and aromatic protons. This sample contained comparable amounts of NMP to that of the 5HR-25 sample. The outcome was that it took unusually long, *i.e.* about 7 ms, for the spin diffusion spectra to achieve a stable lineshape; moreover the stabilized spectra did not quite correspond to the equilibrium lineshape (asymptotic $\Delta M(t_{sd}) \approx 0.005$ relative to the entire aromatic intensity). Given that the HR-25 aromatic intensity in HR-25 is about ten times the PAG aromatic intensity in 5HR-25 (including the NMP impurity), a similar equilibration behavior for the HR-25 component in the 5HR-25 sample would lead to a changing $\Delta M(t_{sd})$ up to about 7 ms and a $\Delta M(t_{sd}) \approx 0.05$ at 7 ms. From Table 3, that is what we observe. Hence, since the HR-25 sample displays a level of aliphatic/aromatic inhomogeneity comparable to that of the 5HR-25 sample, we conclude that in the HR-25 spectrum, there most likely exists either an inhomogeneous distribution of NMP and/or of the level of derivatization. Less likely, in our opinion, is the possibility that the PAG is aggregating into larger domains.

It is of interest in this context that the 5HR-70 and the 10HR-70 samples showed intimate mixing. These samples both contain NMP levels estimated by ^{13}C intensities at (3 to 4)% by mass implying a quantity of NMP protons somewhere between 1 and 3 times the number of PAG protons. Thus, these aliphatic NMP protons, if phase separated, could prevent the achievement of spin equilibration. The fact that we did not detect such behavior implies two other points. First, *the NMP must also be dispersed well on a molecular level, i.e., not strongly clustered in an NMP-rich phase.* This is consistent with NMP having a strong affinity for at least some of the HR-70 molecules. A second comment is much more qualitative since it critically depends on one assumption and on differences in $\Delta M(t_{sd})$ of the order of 0.01 to 0.03 as $\Delta M(t_{sd})$ approaches zero. The fine points regarding the NMP preferentially associating with one of the two isomeric forms in HR-0 where those isomers phase separate into large domains are provided in the electronic supplementary information.[†] Therefore, if it can be assumed that the NMP continues to associate preferentially with the one isomer after *t*-BOC derivatizing, then this mixing result implies that the two parent isomers present in HR-0 are reasonably well mixed in the glassy states of 5HR-70 and 10HR-70 in their *t*-BOC-derivatized forms.

The 5tBR-70, 5PB-100 and 10PB-100 samples in Table 3 all showed spin diffusion behaviors, similar to each other, and

characterized by a slightly elevated (≈ 0.03) level of $\Delta M(t_{sd})$ at longer t_{sd} , compared to samples with intimate mixing. Such behavior is characteristic of PAG which, while certainly not clustered into large PAG-rich regions, is intimately mixed with the matrix while simultaneously exhibiting substantial variations in MG/PAG stoichiometry over distances greater than 20 nm. Each of these samples had negligible levels of NMR-detected impurities, so the non-ideal behavior is necessarily a result of compositional inhomogeneities in the PAG or in the matrix.

It is most likely that all three of the foregoing samples are thermodynamically compatible and that the most plausible explanation for the non-ideal behavior is that variations in concentration of PAG and MG arise from differential solubility of PAG and MG in the solvents used. Our reasoning follows: for the 5tBR-70 sample, we first note that the 10tBR-70 sample shows normal behavior (implied thermodynamic compatibility). If incompatibility were present and a PAG rich phase was forming and responsible for the long-time value of $\Delta M(t_{sd})$ for sample 5tBR-70, then the implication is that the 5% PAG composition is very close to the two-phase boundary composition. If so, a much larger portion of the 10tBR-70 sample should phase separate into a PAG-rich phase; but that did not happen. Hence, we look for an alternate explanation for inhomogeneous PAG distribution. Differential solubility is such a possibility. It might seem very speculative to invoke the importance of differential solubility for the 5tBR-70 sample and not for the 10tBR-70 sample. We did not do further experiments to resolve this contrasting spin diffusion behavior.

Explanations for the 5PB-100 and the 10PB-100 follow a similar argument, namely, that tails of the spin diffusion curves for both materials are identical (Table 3). Again the argument can be made that the 10PB-100 should be a lot less mixed than the 5PB-100 sample if phase separation were controlled by thermodynamic incompatibility. Thus, we expect that an explanation like differential solubility also explains the inhomogeneity found in these samples.

A summary of the conclusions about mixing are collected in the remarks in Table 3. The major conclusion of the spin diffusion work is that in the bulk phase, there is thermodynamic compatibility of the PAG with all the MGs studied herein at the PAG concentrations given in Table 1 with the single caveat that the demonstration of compatibility is less strong and not beyond question for 5HR-25, owing to large NMP impurity content.

Inferences about the uniformity of PAG concentration

One would expect that thermodynamic compatibility leads to a uniform concentration of PAG in the MG. The *uniformity* of PAG concentration throughout the sample is very difficult to determine when the PAG proton fraction is so small since it is generally only in the last couple of percent of change in $\Delta M(t_{sd})$, at longer t_{sd} , that one begins to ascertain how uniform the mixing is. For example, if $N_{PAG}/N_{MG} = 1 : 50$, typical of a 95/5 mixture, then eqn (1) and (2) deduce that only the last 2% of the expected change in PAG polarization would convey information that the PAG was dispersed in more than 50% of the MG. In contrast, these experiments are more capable of detecting whether PAG forms larger (>20 nm) domains. Indeed, for every fraction, f , of PAG so sequestered into a pure-PAG phase, the corresponding

asymptote of $\Delta M_s(t_{sd})$ will approach f . Thus, from Table 3, only the 5HR-25 and 5tBR-25 samples even have a chance that as much as 5% is a pure PAG phase.

Samples exhibiting strong hydrogen bonds

Berglund,³⁶ *et al.* have demonstrated a non-linear correlation of the isotropic chemical shift of protons involved in H-bonds with corresponding internuclear O···O distances. The correlations mainly involved acid protons, both organic and inorganic. Moreover, the correlation was monotonic, such that a reduction in O···O distance resulted in a shift downfield. Shorter H-bonds imply stronger interactions.

In Fig. 5, CRAMPS spectra of the 10 unmixed samples studied are shown. Of note are the downfield (8 ppm to 12 ppm) resonances of the HR-0, TS-0 and, to a lesser extent, the PB-0 and the HR-25 samples. From the correlation curve of Berglund,³⁶ resonances falling in this range, on average would correspond to O···O distances in the 0.30 nm to 0.27 nm range. Not all of the hydroxyl protons participate in these stronger H-bonds; the remaining are hidden under the aromatic resonances. From

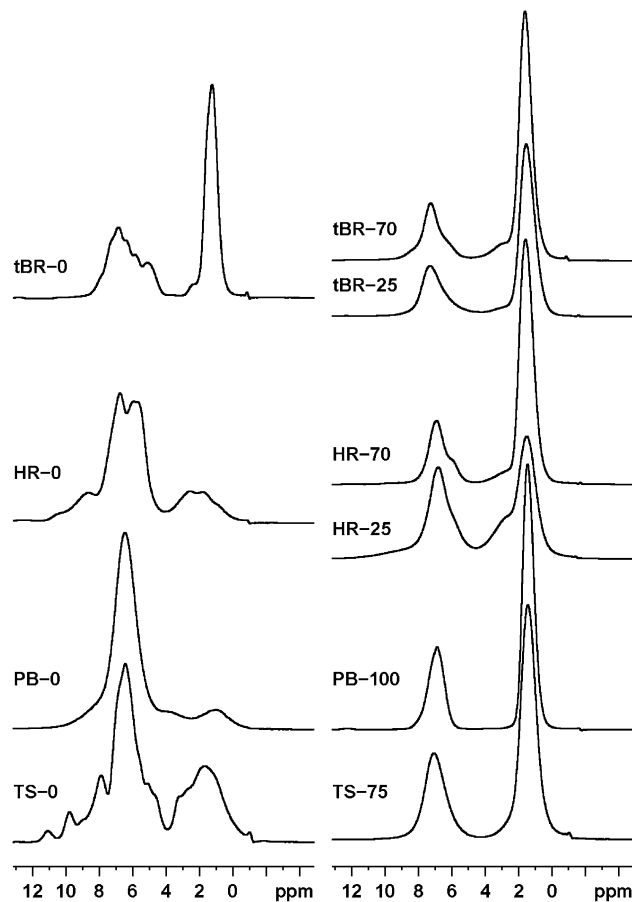


Fig. 5 300 MHz Proton CRAMPS spectra of all of the PAG-free samples. Note the downfield wings in the left column, indicative of strong H-bonding, for all but the tBR-0 sample. Also in the left column, note the better resolution, supporting crystallinity, for all but the PB-0 sample. One can also see aliphatic resonances (0 ppm to 5 ppm) from the ethyl acetate contamination in PB-0.

Fig. 5 one would also conclude that the glassy t-BOC derivatives of HR and TS interfere with the formation of these stronger H-bonds since no such downfield resonances appear. Moreover, H-bonds which form in the tBR-0 sample are all of the weaker variety. The strength of the H-bonds may influence the solubility of a material in a given solvent; hence, it is a speculative consideration that, in using HR or TS materials as photoresists, one should try to avoid full deprotection so as to minimize the probability of strong H-bond formation, especially accompanied by crystallization, during the post-exposure-baking period. Strong H-bonds and/or crystallization could imply a slower solubilization during development. It might thus follow, based on statistics alone, that HR-70 could be superior in this regard to TS-75 in that it would appear less likely that partial deprotection would strip all of the 8 or 9 t-BOC residues from a HR-70 molecule *versus* all of the 2 or 3 residues from a TS-75 molecule.

We note, in connection with the lineshapes of Fig. 5, that spectra of all the protected samples are characterized by well separated regions on either side of ≈ 4.5 ppm; thus aliphatic and (aromatic + hydroxyl) intensities are well separated. This allows us to check on the level of t-BOC substitution since such substitution increases the aliphatic fraction. Those results are given in Table 2. While the TGA and the NMR estimates of protection levels agree, within experimental error, for over half of the samples, there are also notable exceptions, namely, for tBR-70 where the NMR results are 9% lower than TGA and for TS-75 where NMR results are 19% higher. Also, both NMR and TGA suggest that the tBR25 sample has a protection level in (30 to 35)% by mol range rather than 25%. The NMR-measured uncertainties for the HR25 and HR70 samples are higher than average since those samples have a considerable amount of NMP. Corrections for the presence of NMP were made based on the amount of NMP seen in the less-quantitative ^{13}C spectra.

Experimental[‡]

Materials

Chemicals were purchased from Sigma-Aldrich unless otherwise stated and used without further purification. Anhydrous or HPLC grade solvents were used unless otherwise stated. Syntheses of calix[4]resorcinarene derivatives (HR-n and tBR-n) were performed according to published reports.^{4,6,10} TPS-PFBS was purchased from Aldrich and used as received. Synthesis and TGA analysis took place at Cornell and NMR experiments and analysis were done at NIST.

HR-0. 10 g (0.09 mol) of resorcinol and 11 g (0.09 mol) of 4-hydroxy benzaldehyde were dissolved in 80 mL ethanol. 10 mL of concentrated hydrochloric acid was also added to the reaction mixture. The reaction solution was stirred under reflux at 80 °C

for 8 h. A pink solid began to precipitate from the homogeneous mixture after about 2 h.

The precipitate was collected with a glass filter, washed with ethanol and dried under vacuum at 50 °C overnight to remove any trapped solvent. Yield = 75%.

tBR-0. 10 g (0.09 mol) of resorcinol and 14.6 g (0.09 mol) of 4-tert-butyl benzaldehyde were dissolved in 80 mL ethanol. 10 mL of concentrated hydrochloric acid was also added to the reaction mixture. The reaction solution was stirred under reflux at 80 °C for 8 h. A light orange solid began to precipitate from the homogeneous mixture after about 2 h.

The precipitate was collected with a glass filter, washed with ethanol and dried under vacuum at 50 °C overnight to remove any trapped solvent. Yield = 65%.

TS-0. This material was commercially obtained from TCI America (Portland, OR, USA) and used without further purification.

PB-0. HPB was synthesized in a three step method as published.³⁷

t-BOC protection of calix[4]resorcinarene derivatives

Derivatization of tBR-25 and tBR-70 followed literature procedures.³⁷ The protected samples were purified using column chromatography containing silica support (230 to 400 mesh) with acetone as the eluent. Purification of the protected compound is very important in removing minor impurities that affect thermal and lithographic properties of this material. HR-0 was not soluble in common organic solvents. Hence, NMP was used as the reaction solvent for t-BOC protection. HR-25 and HR-70 samples were obtained *via* precipitation in water. The samples were then purified through column chromatography using acetone. Due to the high boiling point of NMP, some residual solvent was observed in the HR-25 and HR-70 samples even after drying in vacuum overnight at 50 °C. tBR-0 was easily soluble in common organic solvents; hence, t-BOC protection of this material was done in acetone. The products tBR-25 and tBR-70 were extracted with ethyl acetate and purified through column chromatography using acetone. TS-0 and PB-0 were protected according to literature procedures.³⁷ TS-75 was purified using an acetone column. PB-100 was purified using a CH_2Cl_2 column.

NMR spectroscopy

All spectra were taken at ambient temperature. 300 MHz proton spectra were taken using a Bruker Avance spectrometer (Bruker Biospin, Inc., Billerica, MA, USA) equipped with a low-proton-background CRAMPS probe manufactured by Doty Scientific, (Columbia, SC, USA); the probe utilizes 5 mm-OD silicon nitride rotors. The proton radiofrequency power level gave nutation frequencies of 167 kHz ($1.5 \mu\text{s}$ 90° pulses). The specific chemical-shift-based spin diffusion (CSBSD) experiment that we used has been described previously¹⁵ as has its interpretation.²⁶ The MREV8 multiple pulse sequence^{20,21} was employed with a $3.3 \mu\text{s}$ subcycle time leading to a $39.6 \mu\text{s}$ cycle time. Magic angle

[‡] Certain commercial equipment and materials are identified in this paper in order to specify adequately the experimental procedure. In no case does such identification imply recommendations by the National Institute of Standards and Technology nor does it imply that the material or equipment identified is necessarily the best available for this purpose.

spinning rates were chosen to be 2525 Hz so that, in the initial stage of the CSBSD experiment where the magnetization gradients are prepared, the 10 or 20 MREV8 cycles used would correspond to exactly 1 or 2 periods of the rotor. This choice minimizes artifacts. Block-averaging of spin diffusion spectra was employed in order to minimize the impact of any spectrometer drift.

For each sample, the Bloch-decay response to a single excitation pulse was also collected and Fourier transformed to give the normal broadline spectrum. Linewidths for the HR-0, PB-0 and TS-0 samples all were in the 30 kHz to 35 kHz range; however, the remaining samples had linewidths in the range from 13 kHz to 18 kHz owing to the contributions and numerical dominance of the motionally narrowed *t*-butyl protons of the t-BOC group. In addition to the Bloch-decay spectra, T_1^H was also estimated from the zero-crossing time after an inversion-recovery sequence.³⁸ While T_1^H is sensitive to local magnetic fluctuations (molecular motions) and their spectral density at frequencies near 1 GHz, our interest in T_1^H was mainly for two other reasons since we made no effort to exclude oxygen from our samples and the latter is known to affect solid state T_1^H values for aromatic compounds.^{39,40} First, T_1^H relaxation competes with spin diffusion in producing intensity changes in the CSBSD experiment and we needed to know how competitive it was. All derivatized materials had T_1^H 's in the range from 300 ms to 400 ms; undervatized materials had T_1^H 's about twice as long. Hence, T_1^H processes, over the critical spin diffusion time of 7 ms contributed only a 2% reduction in total intensity. Secondly, the measurement we conducted was capable of identifying the presence of multiple large (>50 nm) phases (*e.g.* in HR-0) in the event that each phase had a different T_1^H . As magnetization recovers after inversion, the lineshape in the vicinity of the zero-crossing, if differing in anything but magnitude from the equilibrium lineshape, indicated the presence of multiple phases. Only HR-0 showed multiple phases in this sense (see supplementary information).†

^{13}C spectra were obtained on a non-commercial spectrometer operating at 2.35 T (25.2 MHz for ^{13}C and 100.2 MHz for protons). Cross polarization (CP) in combination with magic angle spinning (MAS) yielded CPMAS⁴¹ spectra. The probe was non-commercial and included a MAS rotor/stator manufactured by Doty Scientific, Inc. Samples in 7 mm-OD zirconia rotors were spun at 4 kHz, which was sufficient to keep all spinning sidebands out of the region of the centerbands in these spectra. Radio frequency fields corresponded to nutation frequencies of 69 kHz for ^{13}C nuclei and 65 kHz for protons. Continuous-wave decoupling was used. The cross polarization time was 2 ms and usually (5000 to 10000) scans were collected for each spectrum.

Chemical shift scales for ^{13}C were referenced, by substitution, to the methine resonance of adamantane at 29.5 ppm and the shift scale for the CRAMPS spectra was referenced to tetramethylsilane at 0 ppm by substitution. Since variations in sample tuning for CRAMPS spectra can cause shifts, the uncertainty in the placement of the 0 ppm location was ± 0.5 ppm; for ^{13}C spectra, the corresponding uncertainty was ± 0.2 ppm.

NMR samples were all placed in the vacuum oven for at least 24 h at 40 °C prior to analysis.

Quoted uncertainties in measured quantities, unless otherwise specified, correspond to one standard deviation.

Conclusion

The PAG, triphenylsulfonium perfluorobutanesulfonate, was blended with three different architectures of molecular glasses (MGs). Proton spin diffusion methods were used to probe the intimacy of mixing in blends containing (5 or 10)% by mass PAG. The majority of samples were deduced to be thermodynamically compatible on the basis of (a) the spin diffusion data giving a conservatively established upper limit of 3.8 nm diameter for any phase separated PAG domains (assumed spherical), and (b) the argument that thermodynamically driven phase separation of incompatible materials in the presence of slow solvent evaporation is not consistent with the formation of such small domains.

The issue of thermodynamic compatibility of PAG and MGs is an important recognition. However, compatibility alone does not insure that the PAG and MGs will be uniformly mixed throughout any given sample since differential solubility in the common solvent is another possible source for stoichiometric variations across the sample. For the mixtures studied herein, where the PAG exists in minor concentration, the spin diffusion method is quite limited in assaying the *uniformity* of the PAG distribution in the MG matrices. In fact, differential solubility was invoked in a few samples that showed slightly shifted asymptotic behavior for their spin diffusion profiles. Nevertheless, even in the presence of differential solubility, there is a very practical advantage to knowing of thermodynamic compatibility because that knowledge may allow one to get better performance by changing solvent rather than changing MG or PAG.

It was seen that some of the undervatized precursor materials for these MGs are crystalline and form strong hydrogen bonds. As these MGs are processed in a photoresist application, it is, in principle, possible that completely deprotected MG molecules form, which, in turn could lead to the formation of crystallites. The introduction of isomers is one approach for suppressing crystallization, as in the PB-0 system.

The PB-100/PAG samples showed the most consistent tendency to exhibit inhomogeneous composition, probably owing to differential solubility. That tendency should be considered during spin coating in photoresist applications. The inclusion of the tBR-25 and HR-25 samples was intended to probe whether there was a substantial change in compatibility of PAG and MG as one lowered the number of t-BOC groups, just as one might do during the post apply baking process. We did not see such an unambiguous indication of incompatibility.

Conclusions, not included herein but described in the supplemental materials, are as follows. One of the resorcinarenes (HR-0), which consisted of two stereoisomers, was seen to have a special affinity for the solvent, NMP, such that the most symmetric isomer in this crystalline material cocrystallized with NMP as a 1 : 1 adduct. After t-BOC protection the MG still had a strong affinity for the NMP; however, the interaction between NMP and the parent isomer is different from the interaction between NMP and the protected MG in the sense that at least the orientation of the ^{14}N quadrupolar tensor on the NMP molecule changes. Finally, all t-BOC protected MGs are glassy while 3 of the 4 undervatized materials are crystalline. The fourth, PB-0, probably has 2-dimensional order. The undervatized samples, with the exception of tBR-0, all displayed some very strong H-bonds whose protons resonated downfield from the aromatic resonances.

Finally, the thermodynamic compatibility of this PAG with these molecular glasses and with other polymers is interesting in itself from the point of view that the PAG is a molecular salt that has characteristics of high polarity, a perfluorinated portion, charge localization and possibilities for π - π -bonding. It is not immediately obvious which of these characteristics foster compatibility. Hence, it seems reasonable to ask whether thermodynamic compatibility implies that the molecules are dispersed as individual molecules or in smaller clusters of say, 3 to 6 molecules where some sequestering from the matrix of less compatible portions of the molecules is possible. This would also be interesting from the point of view of thinking about the diffusion of PAG and the breakup of the clusters during the post-exposure baking step in a typical photoresist process. A possible NMR approach to addressing this possibility of small clusters is to look for clustering *via* multiple quantum coherences for ^{19}F nuclei.⁴² The objective would be to look for higher-order multiple-quantum coherences (arising from a network of dipolar-coupled ^{19}F spins) characteristic of more than just the nine ^{19}F atoms associated with a single PAG molecule.

Disclaimer

Official contribution of the National Institute of Standards and Technology; not subject to copyright in the United States.

Acknowledgements

V.M.P. and D.L.V. acknowledge support by a cooperative research and development agreement between Intel Corporation and NIST (NIST CRADA #CN-1893). We also would like to recognize Kwang-Woo Choi, Manish Chandhok, Wang Yueh, Todd Younkin, Melissa Shell, George Thompson, and Christof Krautschik from Intel, and Eric Lin from NIST for their interest and support. The Cornell authors thank Semiconductor Research Corporation (SRC) and Intel Corporation for funding. The Cornell Nanoscale Science and Technology Facility (CNF) and the Cornell Center for Materials Research (CCMR) are thanked for use of their facilities.

References

- 1 M. Yoshiwa, H. Kageyama, Y. Shirota, F. Wakaya, K. Gamo and M. Takai, *Applied Physics Letters*, 1996, **69**, 2605.
- 2 T. Kadota, H. Kageyama, F. Wakaya, K. Gamo and Y. Shirota, *Journal of Photopolymer Science and Technology*, 1999, **12**, 375.
- 3 T. Kadota, H. Kageyama, F. Wakaya, K. Gamo and Y. Shirota, *Chemistry Letters*, 2004, **33**, 706.
- 4 O. Haba, K. Haga, M. Ueda, O. Morikawa and H. Konishi, *Chemistry of Materials*, 1999, **11**, 427.
- 5 N. M. Felix, A. De Silva, C. M. Y. Luk and C. K. Ober, *Journal of Materials Chemistry*, 2007, **17**, 4598.
- 6 L. M. Tunstad, J. A. Tucker, E. Dalcanale, J. Weiser, J. A. Bryant, J. C. Sherman, R. C. Helgeson, C. B. Knobler and D. J. Cram, *Journal of Organic Chemistry*, 1989, **54**, 1305.
- 7 F. Weinelt and H. J. Schneider, *Journal of Organic Chemistry*, 1991, **56**, 5527.
- 8 K. Young-Gil, J. B. Kim, T. Fujigaya, Y. Shibasaki and M. Ueda, *Journal of Materials Chemistry*, 2002, **12**, 53.
- 9 M. Ueda, D. Takahashi, T. Nakayama and O. Haba, *Chemistry of Materials*, 1998, **10**, 2230.
- 10 D. Bratton, R. Ayothi, N. Felix, H. B. Cao, H. Deng and C. K. Ober, *Proceedings SPIE*, 2006, **6153**, 61531D.
- 11 D. Bratton, R. Ayothi, H. Deng, H. B. Cao and C. K. Ober, *Chemistry of Materials*, 2007, **19**, 3780.
- 12 S. W. Chang, R. Ayothi, D. Bratton, D. Yang, N. Felix, H. B. Cao, H. Deng and C. K. Ober, *Journal of Materials Chemistry*, 2006, **16**, 1470.
- 13 D. Yang, S. W. Chang and C. K. Ober, *Journal of Materials Chemistry*, 2006, **16**, 1693.
- 14 J. Y. Dai, S. W. Chang, A. Hamad, D. Yang, N. Felix and C. K. Ober, *Chemistry of Materials*, 2006, **18**, 3404.
- 15 G. C. Campbell and D. L. VanderHart, *Journal of Magnetic Resonance*, 1992, **96**, 69.
- 16 P. Caravatti, P. Neuenschwander and R. R. Ernst, *Macromolecules*, 1985, **18**, 119.
- 17 M. Goldman and L. Shen, *Physical Review*, 1966, **144**, 321.
- 18 K. Schmidt-Rohr and H. W. Spiess, in *Multidimensional Solid State NMR and Polymers*, Academic Press, London, 1994, ch. 13.
- 19 D. L. VanderHart, V. M. Prabhu and E. K. Lin, *Chemistry of Materials*, 2004, **16**, 3074.
- 20 P. Mansfiel, M. J. Orchard, D. C. Stalker and K. H. Richards, *Physical Review B*, 1973, **7**, 90.
- 21 W. K. Rhim, D. D. Elleman and R. W. Vaughan, *Journal of Chemical Physics*, 1973, **59**, 3740.
- 22 E. R. Andrew and E. Szczesniak, *Progress in Nuclear Magnetic Resonance Spectroscopy*, 1995, **28**, 11.
- 23 I. J. Lowe, *Physical Review Letters*, 1959, **2**, 285.
- 24 L. M. Ryan, R. E. Taylor, A. J. Paff and B. C. Gerstein, *Journal of Chemical Physics*, 1980, **72**, 508.
- 25 A. Abragam, in *The Principles of Nuclear Magnetism*, Oxford University Press, London, 1961, ch. V.
- 26 D. L. VanderHart and G. B. McFadden, *Solid State Nuclear Magnetic Resonance*, 1996, **7**, 45.
- 27 E. L. Jablonski, V. M. Prabhu, S. Sambasivan, E. K. Lin, D. A. Fischer, D. L. Goldfarb, M. Angelopoulos and H. Ito, *Journal of Vacuum Science & Technology B*, 2003, **21**, 3162.
- 28 J. L. Lenhart, R. L. Jones, E. K. Lin, C. L. Soles, W. L. Wu, D. A. Fischer, S. Sambasivan, D. L. Goldfarb and M. Angelopoulos, *Journal of Vacuum Science & Technology B*, 2002, **20**, 2920.
- 29 J. L. Lenhart, D. A. Fischer, S. Sambasivan, E. K. Lin, R. L. Jones, C. L. Soles, W. L. Wu, D. L. Goldfarb and M. Angelopoulos, *Langmuir*, 2005, **21**, 4007.
- 30 V. M. Prabhu, S. Sambasivan, D. Fischer, L. K. Sundberg and R. D. Allen, *Applied Surface Science*, 2006, **253**, 1010.
- 31 W. E. Wallace, K. M. Flynn, C. M. Guttman, D. L. VanderHart, V. M. Prabhu, A. De Silva, N. M. Felix, and C. K. Ober, in preparation.
- 32 J. Crank, in *The Mathematics of Diffusion*, Oxford University Press, London, 1957.
- 33 D. L. VanderHart, *Macromolecules*, 1994, **27**, 2837.
- 34 K. A. Laverty, B. D. Vogt, V. M. Prabhu, E. K. Lin, W. L. Wu, S. K. Satija and K. W. Choi, *Journal of Vacuum Science & Technology B*, 2006, **24**, 3044.
- 35 R. L. Jones, T. J. Hu, E. K. Lin, W. L. Wu, D. L. Goldfarb, M. Angelopoulos, B. C. Trinque, G. M. Schmid, M. D. Stewart and C. G. Willson, *Journal of Polymer Science Part B-Polymer Physics*, 2004, **42**, 3063.
- 36 B. Berglund and R. W. Vaughan, *Journal of Chemical Physics*, 1980, **73**, 2037.
- 37 M. M. Hansen and J. R. Riggs, *Tetrahedron Letters*, 1998, **39**, 2705.
- 38 T. C. Farrar and E. D. Becker, in *Pulse and Fourier Transform NMR*, Academic Press, New York, 1971, pp. 20–22.
- 39 D. Capitani, A. L. Segre and J. S. Blacharski, *Macromolecules*, 1995, **28**, 1121.
- 40 D. Capitani, C. Derosa, A. Ferrando, A. Grassi and A. L. Segre, *Macromolecules*, 1992, **25**, 3874.
- 41 J. Schaefer, E. O. Stejskal and R. Buchdahl, *Macromolecules*, 1975, **8**, 291.
- 42 S. J. Limb, B. E. Scruggs and K. K. Gleason, *Macromolecules*, 1993, **26**, 3750.